Video Article

In Situ Neutron Powder Diffraction Using Custom-made Lithium-ion Batteries

William R. Brant[1], Siegbert Schmid[1], Guodong Du[2], Helen E. A. Brand[3], Wei Kong Pang[2,4,5], Vanessa K. Peterson[4], Zaiping Guo[2,5], Neeraj Sharma[6]

[1]School of Chemistry, University of Sydney

[2]Institute for Superconducting & Electronic Materials, University of Wollongong

[3]Australian Synchrotron

[4]Australian Nuclear Science and Technology Organisation

[5]School of Mechanical, Materials, and Mechatronic Engineering, University of Wollongong

[6]School of Chemistry, University of New South Wales

Correspondence to: Neeraj Sharma at neeraj.sharma@unsw.edu.au

URL: https://www.jove.com/video/52284
DOI: doi:10.3791/52284

Keywords: Physics, Issue 93, In operando, structure-property relationships, electrochemical cycling, electrochemical cells, crystallography, battery performance

Date Published: 11/10/2014

Citation: Brant, W.R., Schmid, S., Du, G., Brand, H.E., Pang, W.K., Peterson, V.K., Guo, Z., Sharma, N. *In Situ* Neutron Powder Diffraction Using Custom-made Lithium-ion Batteries. *J. Vis. Exp.* (93), e52284, doi:10.3791/52284 (2014).

Abstract

Li-ion batteries are widely used in portable electronic devices and are considered as promising candidates for higher-energy applications such as electric vehicles.[1,2] However, many challenges, such as energy density and battery lifetimes, need to be overcome before this particular battery technology can be widely implemented in such applications.[3] This research is challenging, and we outline a method to address these challenges using *in situ* NPD to probe the crystal structure of electrodes undergoing electrochemical cycling (charge/discharge) in a battery. NPD data help determine the underlying structural mechanism responsible for a range of electrode properties, and this information can direct the development of better electrodes and batteries.

We briefly review six types of battery designs custom-made for NPD experiments and detail the method to construct the 'roll-over' cell that we have successfully used on the high-intensity NPD instrument, WOMBAT, at the Australian Nuclear Science and Technology Organisation (ANSTO). The design considerations and materials used for cell construction are discussed in conjunction with aspects of the actual *in situ* NPD experiment and initial directions are presented on how to analyze such complex *in situ* data.

Video Link

The video component of this article can be found at https://www.jove.com/video/52284/

Introduction

Rechargeable lithium-ion batteries provide portable energy for modern electronics and are important in high-energy applications such as electric vehicles and as energy storage devices for large-scale renewable energy generation.[3-7] A number of challenges remain to achieve widespread use of rechargeable batteries in vehicular and large-scale storage, including energy densities and safety. The use of *in situ* methods to probe atomic and molecular-scale battery function during operation are becoming increasingly common as the information gained in such experiments can direct methods to improve existing battery materials, *e.g.* by identifying possible failure mechanisms,[8-10] and by revealing crystal structures that could be considered for the next generation of materials.[11]

A primary goal of *in situ* NPD is to probe the crystal structure evolution of the components inside a battery as a function of charge/discharge. In order to measure the crystal structure evolution the components must be crystalline, which focuses such studies on crystallographically-ordered electrodes. It is at the electrodes that the charge carrier (lithium) is inserted/extracted and such changes are followed by NPD. *In situ* NPD offers the possibility to "track" not only the reaction mechanism and lattice parameter evolution of the electrodes, but also the insertion/extraction of lithium from the electrodes. Essentially the charge carrier in lithium-ion batteries can be followed. This gives a lithium-centered view of the battery function and has been recently demonstrated in only a few studies.[11-13]

NPD is an ideal technique to examine lithium-containing materials and lithium-ion batteries. This is because NPD relies on the interaction between a neutron beam and the sample. Unlike X-ray powder diffraction (XRD), where the interaction of the X-ray radiation is predominantly with the electrons of the sample and thus varies linearly with atomic number, in NPD the interaction is mediated by neutron-nuclei interactions that result in a more complex and apparently random variation with atomic number. Thus, *in situ* NPD is particularly promising for the study of lithium-ion battery materials due to factors such as the sensitivity of NPD towards lithium atoms in the presence of heavier elements, the non-destructive interaction of neutrons with the battery, and the high penetration depth of neutrons enabling the examination of the bulk crystal-structure of the battery components within whole batteries of the size used in commercial devices. Therefore, *in situ* NPD is particularly useful for the study of lithium-ion batteries as a result of these advantages. Despite this, the uptake of *in situ* NPD experiments by the battery-research community has been limited, accounting for only 25 publications since the first report of using *in situ* NPD for battery research in 1998.[14]

The limited uptake is due to some major experimental hurdles, such as the need to account for the large incoherent neutron-scattering cross section of hydrogen in the electrolyte solutions and separator in the battery, which is detrimental to the NPD signal. This is often overcome by substituting with deuterated (^{2}H) electrolyte solutions and replacing the separator with alternate hydrogen-free or poor materials.[15] Another hurdle is the need to have sufficient sample in the neutron beam, a requirement that often necessitates the use of thicker electrodes which in turn limits the maximum charging/discharging rate that can be applied to the battery. A more practical concern is the relatively small number of world-wide neutron diffractometers relative to X-ray diffractometers, and their capabilities — *e.g.* time and angular resolution. As new neutron diffractometers have come online and the abovementioned hurdles overcome, *in situ* NPD experiments have grown in number.

There are two options to conduct *in situ* NPD experiments, using either commercial or custom-built cells. Commercial cells have been demonstrated to reveal structural information, including the evolution of lithium content and distribution in electrodes.[8-11,16-20] However, using commercial cells limits the number of electrodes that can be studied to those already commercially available, and where manufacturers or select research facilities are engaged to produce commercial-type cells with as yet un-commercialized materials. The production of the commercial-type cells is dependent on the availability of sufficient quantities of electrode material for cell manufacture, typically of the order of kilograms and significantly higher than that used in battery research, which can be a barrier to cell production. Commercial cells typically feature two electrodes that evolve during charge/discharge and the evolution of both electrodes will be captured in the resulting diffraction patterns. This is because the neutron beam is highly penetrating and can penetrate the single lithium-ion cells (*e.g.*, the entire volume of 18,650 cells). The evolution of the two electrodes can make the data analysis complicated, but if sufficient Bragg reflections of both electrodes are observed these can be modeled using whole powder-pattern methods. Nonetheless, custom-made half cells can be constructed in which one electrode is lithium and should not structurally change during charge/discharge and therefore act as an (or another) internal standard. This leaves only one electrode that should exhibit structural change, simplifying data analysis. Care must also be taken to ensure that all electrode reflections of interest are not overlapping with reflections from other components undergoing structural change in the cell. The advantage of a custom-made cell is that components can be swapped to alter reflection positions in diffraction patterns. Furthermore, custom-made cells allow researchers the option to, in principle, improve signal-to-noise ratios and to investigate materials that are made in smaller-scale research batches and thereby permitting the *in situ* NPD study of a larger variety of materials.

To date there have been six electrochemical cell designs for *in situ* NPD studies reported, including three cylindrical designs,[14,15,21,22] two coin-type cell designs[23-26] and a pouch cell design.[12,27] The first cylindrical cell design was limited in use to very low charging/discharging rates due to the large quantities of electrode materials used.[14,21] The roll-over design,[15] detailed below, and modified version of the original cylindrical cell,[22] have overcome many of the problems associated with the first cylindrical design, and can be used for reliably correlating the structure of electrode materials with their electrochemistry. Coin-cell designs for *in situ* NPD also allow similar quantities of electrode materials to be probed relative to the roll-over cell, while featuring subtle differences in terms of construction, applicable charging rates, and cost.[15] In particular, the coin-cell type was recently reported to have been constructed using a Ti-Zn alloy as the casing material (null-matrix) which produces no signal in the NPD patterns.[26] This is similar to the use of vanadium cans in the roll-over design described below. A key factor that can influence applicable charge/discharge rates (and polarization) is electrode thickness, where typically thicker electrodes require the application of lower current. The cell designs that are now becoming more popular are the pouch cells with sheets of multiple individual cells connected in parallel, or sheets that are rolled in a similar manner to the construction of lithium-ion batteries found in mobile electronics.[12,27] This cell is rectangular (a pouch) that can function at higher charge/discharge rates than the roll-over or coin-type cells. In this work, we focus on the 'roll-over' cell design, illustrating the cell construction, use, and some results using the cell.

The electrode preparation for the roll-over design batteries is practically similar to the electrode preparation for use in conventional coin-cell batteries. The electrode can be cast onto the current collector by doctor blading, with the biggest difference being that the electrode needs to span dimensions larger than 35 x 120-150 mm. This can be hard to uniformly coat with every electrode material. Layers of the electrode on current collector, separator, and lithium metal-foil on current collector are arranged, rolled, and inserted into vanadium cans. The electrolyte used is $LiPF_6$, one of the most commonly used salts in lithium-ion batteries with deuterated ethylene carbonate and deuterated dimethyl carbonate. This cell has been used successfully in four reported studies and will be described in greater detail below.[15,28-30]

Protocol

1. Cell Components Required Prior to Construction

NOTE: A vanadium can is conventionally used for NPD experiments and it is a wholly-vanadium tube that is sealed at one end and open at the other. There is virtually no signal in NPD data from vanadium.

1. Cut a piece of lithium metal-foil to dimensions matching the volume of the vanadium can. For example, cut a piece approximately 120 x 35 mm for a 9 mm diameter vanadium can. In addition, use thinner lithium foil to minimize neutron absorption, noting that thicknesses below 125 µm may be difficult to handle without tearing.
2. Pre-select the type of separator to be used. Cut a sheet of separator such that the dimensions are slightly larger than the electrodes, *e.g.* 140 x 40 mm.
   NOTE: While porous polyvinyl-difluoride (PVDF) membrane readily soaks up electrolyte, it is expensive and can be easily damaged and torn if not handled carefully during construction. Alternatively, commercially available polyethylene-based sheets are more robust, however they do not soak up electrolyte as readily and generally reduce the signal-to-noise due to the larger hydrogen content.
3. Make the positive electrode by following the guidelines set out by Marks *et al*.[31] Namely, combine PVDF, carbon black, and the active material at a selected ratio. Typically, use a ratio of 10:10:80 of PVDF:carbon:active material, but adjust this depending on the material under investigation. Grind the mixture and add *n*-methyl pyrrolidone (NMP) dropwise until a slurry forms, then stir overnight.
4. Spread the mixture onto aluminum foil (20 µm thickness) using the doctor blade technique.
   1. Adhere the current collector sheet of dimensions 200 x 70 mm to a smooth surface (*e.g.* glass) by applying a few drops of ethanol on to the surface and placing the current collector on the surface. Alternatively, use an instrument which can pull a slight vacuum on the current collector from the smooth surface. Smooth out the current collector to ensure that there are no crinkles or creases prior to applying the slurry.

2. Place a tooth or wide semi-circle shaped puddle of the slurry on one end of the current collector. Using a notch bar, roller or specially designed coater (a notch bar with a pre-defined height above the current collector, *e.g.* 100 or 200 µm is typically used) spread the slurry over the current collector by sliding the chosen device across the current collector and slurry, resulting in the spreading of the slurry onto the current collector surface.
3. Gently remove the current collector from the smooth surface and place the current collector and spread slurry into a vacuum oven for drying.
   NOTE: The spreading technique is described in greater detail in Marks *et al.*[31]

5. Cut the positive electrode prepared in step 1.3 such that the dimensions match the lithium foil. Ensure that there is a "tab" of uncoated metal current collector approximately 0.5 cm in length at one end. To improve battery performance, press the dried positive electrode film into the current collector using a flat plate press.
   NOTE: **Figure 1** shows the relative sizes of the separator and positive electrode components. Minimum active material quantity in the electrode is 300 mg, however, the larger the quantity (relative to other battery components), the better the NPD signal. A larger signal may allow more detailed information to be extracted from the NPD data and better temporal resolution.
6. Pre-prepare 1 M lithium hexafluorophosphate in a 1/1 vol% mixture of deuterated ethylene carbonate and deuterated dimethyl carbonate. Ensure that all the $LiPF_6$ is dissolved and the electrolyte is thoroughly mixed prior to use.
7. Cut a piece of current collector of the same dimensions as the positive electrode in step 1.5 and weigh the current collector and positive electrode. Subtract these masses to obtain the mass of the electrode mixture. Multiply the mass of the electrode mixture by 0.8 to give the mass of the active material.

2. Cell Construction

1. Prior to assembling the cell inside an argon filled glovebox, lay down either a plastic tray or some other non-metallic covering on the base of the gloxebox.
2. Stack the individual components in the following order: A long strip of separator, positive electrode with the slurry facing up and aluminum rod (or copper wire) wound in the "tab" at one end, the second strip of separator, and finally the lithium metal with copper wire wound on the end of the lithium metal (the same end as the aluminum rod).
3. Start rolling the layers from the end with the aluminum rod and copper wire, ensuring that the two electrodes do not come into contact.
4. If a polyethylene-based sheet was selected as the separator, occasionally add several drops of electrolyte to the separator between the lithium metal and positive electrode along the entire length of the stack. Alternatively, add the drops gradually during the rolling process. If PVDF membrane was used as the separator this step is not necessary.
5. Take care to ensure that the electrode is rolled tightly and that the layers remain aligned.
   NOTE: If the layers become misaligned the rolling process may need to be restarted, however, caution must be taken as the electrolyte solution is highly volatile and more may need to be added.
6. Ensure that the longer piece of separator completely wraps around the stack or roll such that the electrodes are not exposed (*i.e.* the electrodes don't touch the vanadium housing).
7. Insert the rolled stack into the vanadium can such that the copper wire and aluminum rod protrude 2-3 cm beyond the top of the vanadium can. Add the remaining electrolyte dropwise into the top of the vanadium can, use 1.5 ml in total.
8. Add a rubber stopper with notches cut in the sides for the aluminum rod and copper wire into the top of the vanadium can. Seal the can by melting dental wax over the top of the can and around the end of the plastic sheath of the copper wire. Check that the final cell appears as shown in **Figure 2**.
9. Allow the cell to "age" or "wet" horizontally for 12-24 hr. Prior to use, test the open-circuit potential by connecting the aluminum rod and the copper wire to the terminals of a multi-meter and measuring the potential of the constructed cell. Also ensure that there are no leaks by visual inspection.

Representative Results

We have demonstrated the versatility in using this roll-over cell in the literature[15,28-30] and here we present an example with the $Li_{0.18}Sr_{0.66}Ti_{0.5}Nb_{0.5}O_3$ electrode.[32]

Prior to attempting a sequential Rietveld refinement (Rietveld refinements as a function of state-of-charge), a single refinement of a multiphase model to the first data set was performed, with this data collected for the pristine cell prior to current application. Several models were tested to determine which structural parameters could be accurately refined. Ideally, all structural parameters would be refined using the first pattern and also during the sequential refinements. However, occasionally this may not be possible due to factors such as a lower signal-to-noise, which is especially important for tracking small changes to the lithium position and occupancy, and peak overlap. In the present case to obtain a stable model parameters which were strongly correlated (based on the correlation matrix) were not refined. That is, all the cation atomic displacement parameters were fixed to values obtained from *ex-situ* measurements. Such restrictions have often been necessary for the "roll-over" *in-situ* cell design.[11,29,30] The final outcome of the multiphase Rietveld refinement of the $Li_{0.18}Sr_{0.66}Ti_{0.5}Nb_{0.5}O_3$, copper, and lithium metal structures is shown in **Figure 3**. The resulting structural data are provided in **Table 1**. The reason for the large Bragg R value in the refinement compared to the low χ^2 value is likely due to the relatively large proportions of weak reflections in both the main and lithium-metal phase, which are strongly influenced by the background in the data. As the background is quite irregular, and therefore difficult to accurately model, these weaker reflections also become difficult to accurately model.

The refinement result prior to cell discharge provides a basic indication of what may be refined sequentially. However, following the progression of refineable parameters during cycling is not the only way to track structural change during discharge. Changes in intensity of specific characteristic reflections, the appearance of new reflections, and cell parameter variations as a function of discharge can provide significant information concerning the structural changes which take place during discharge. Sequential fitting of a single reflection within each diffraction pattern collected can be performed in programs such as LAMP[33] and Origin. Further, as the diffraction patterns and electrochemical data are collected simultaneously they can both be plotted together as a function of time. The electrochemical procedure followed during the *in situ*

experiment performed on $Li_{0.18}Sr_{0.66}Ti_{0.5}Nb_{0.5}O_3$ is provided in **Table 2**. These conditions provide a reference for the changes observed during electrochemical cycling, as indicated within **Figure 4**.

The first three components from the top of **Figure 4** display the various changes which occur to the 115 reflection during cycling. Under these plots are the change in cell parameter and electrochemical potential profile. An interesting aspect of lithium insertion into $Li_{0.18}Sr_{0.66}Ti_{0.5}Nb_{0.5}O_3$ is that for potentials above 1 V it is reversible, however, discharge below 1 V results in irreversible lithium insertion. For lithium insertion above 1 V, 0.25 mol Li/formula unit can be reversibly inserted under constant current conditions and takes 1,257 min at 1.7(1) mA g^{-1}.[32,34] Under equilibrium conditions (lower current densities) up to 0.4 mol Li/formula unit can be inserted in 160 hr. The insertion of lithium within this region is known to proceed via a solid solution reaction with the unit-cell volume continuously expanding to 1.81(9)% larger following the insertion of 0.25 mol of lithium. In comparison, the volume of the electrode in the neutron cell expanded by only 0.61(6)% in 870 min at 2.5 mA g^{-1}. However, on charging at 5.0 mA g^{-1} the cell contracted further than the initial values, suggesting that self-discharge had occurred before the start of the experiment. Comparing absolute values, the unit cell of a completely charged material (no lithium) was found to be 3.93190(2) Å from synchrotron X-ray diffraction data compared to 3.9345(5) Å from the *in situ* NPD data. Further, the material discharged to 1 V was found to have a unit-cell length of 3.95640(2) Å from synchrotron X-ray diffraction data compared to 3.9454(7) Å from the *in situ* NPD data. Thus it appears as though the material did not completely react on discharge to 1 V, nor on charging. Besides the higher applied current densities, a low pressure applied to the battery stack (or roll) can result in high area-specific impedances and so charge and discharge runs would end prematurely due to high polarization. The latter is a major factor in constructing these cells and it is crucial to obtain a good quality electrode roll for the *in situ* neutron diffraction cell. Further, if the applied pressure is uneven, this could result in the formation of two phases as parts of the cell react faster than others. The only indication that two-phase behavior was occurring was a reversible broadening of the 115 reflection (**Figure 4A** and **B**).

During cycling, the peak intensity of the 115 reflection reduced as more lithium was inserted into the structure and then increased as lithium was removed. Simultaneously, the peak width (full-width at half maximum, FWHM) varies in the opposite sense, resulting in the overall integrated peak intensity remaining constant during lithium insertion and extraction. The same trend occurred for all other observed and fitted reflections. Thus, there were no apparent structural components to the changes in peak intensity. While peak broadening can be associated with a loss of crystallinity or a reduction in particle size, the reversibility of the changes indicate the formation of several phases reacting at different rates. This phase segregation is then strongly enhanced below 1 V with a second phase becoming distinct.

Preliminary electrochemical cycling experiments performed on $Li_{0.18}Sr_{0.66}Ti_{0.5}Nb_{0.5}O_3$ have shown a flat potential output below 1 V, leading to the anticipation that a second phase should appear within this region. It was also hypothesized that this second phase could be the cause of irreversible lithium insertion within this region. The regions where this second phase becomes most visually distinct are indicated with orange bars in **Figure 4**. Within the angular resolution provided by the Wombat diffractometer, the second phase seems to form at the same potential regardless of the discharge current used (2.5 mA g^{-1} for the second discharge, 3.8 mA g^{-1} for the third). As more lithium is inserted into the $Li_{0.18}Sr_{0.66}Ti_{0.5}Nb_{0.5}O_3$ structure the diffusion of lithium into the bulk slows (from 10^{-7} to 10^{-8} cm^2 sec^{-1}).[32] It appears as though the rate of diffusion into the bulk reduces enough to increase the rate of phase segregation during the course of discharge.

While a sequential refinement with a second perovskite phase was not possible due to the similarities of the two phases and resulting peak overlap, consideration of the topographical plot of the 115 reflection (**Figure 4C**) can still provide insight into the structural changes of the positive electrode. In a system at equilibrium, a two-phase region is marked by one phase disappearing at the same rate that a second phase appears as a function of composition (or as a function of any other order parameter, such as temperature), such that their phase fractions always sum to one. However, within the two-phase region observed below 1 V for $Li_{0.18}Sr_{0.66}Ti_{0.5}Nb_{0.5}O_3$ the new phase varies continuously, while the first phase is unchanging. Thus, the *in situ* experiment was able to probe the non-equilibrium behavior of the positive electrode material as a function of state of charge. The second phase stops expanding before the end of discharge. This may signal a shift to an equilibrium two-phase conversion, however, no intensity changes were observed. Changes in the relative intensity of the two reflections were observed once the cell was allowed to relax (the region indicated by the red bar in **Figure 4**). During this time, the reflection at higher 2θ begins to lose intensity relative to the reflection at lower 2θ, indicating that phase equilibration occurs once the applied current has been switched off. A single phase was then rapidly reformed during charging, suggesting that the two-phase reaction is reversible. This prediction was confirmed by discharging below 1 V multiple times. Thus, it is still uncertain why cycling below 1 V results in irreversible lithium insertion. It appears as though the second phase forms as a result of inhibited lithium diffusion into the structure, possibly intrinsically or because of the low pressure applied to the battery stack. It should be noted that the unit cell does not return to its original size on each subsequent charge, implying that some lithium remains within the bulk structure. Cycling the cell below 1 V will require a further experiment where polarization effects are greatly reduced or eliminated. Without polarization as a competing influence, the effect of the changing lithium diffusion within the material and its structural changes below 1 V can be determined.

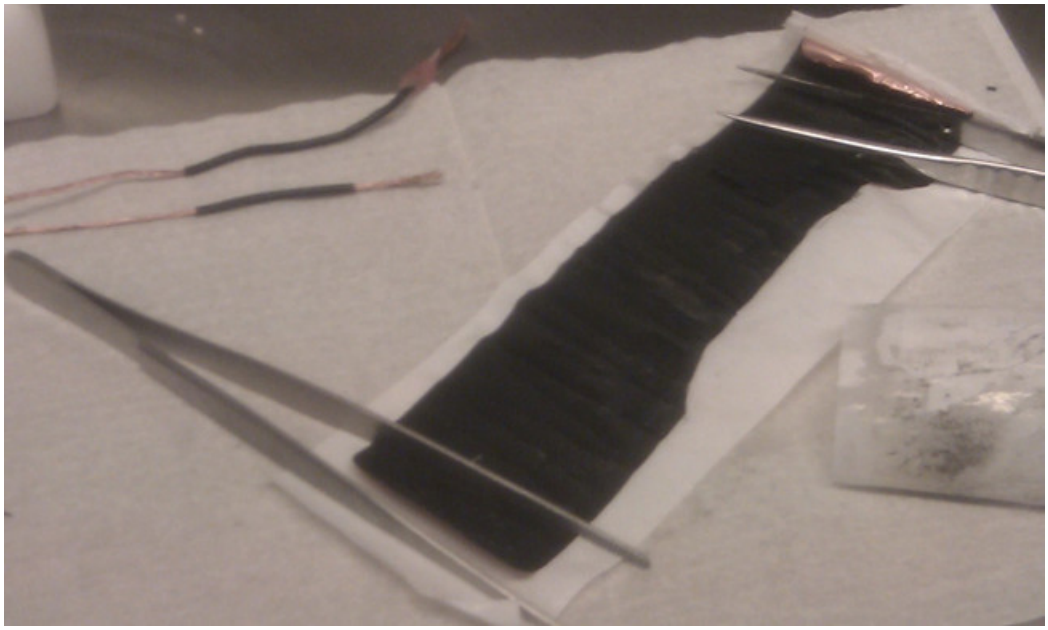

Figure 1: Photo of the positive electrode component on a strip of polyethylene-based separator following extraction from an *in situ* cell. The image demonstrates the relative sizes of positive electrode and separator required to prevent contact between the two electrodes. Also included in the photo are the copper wires which enable connection to an external circuit.

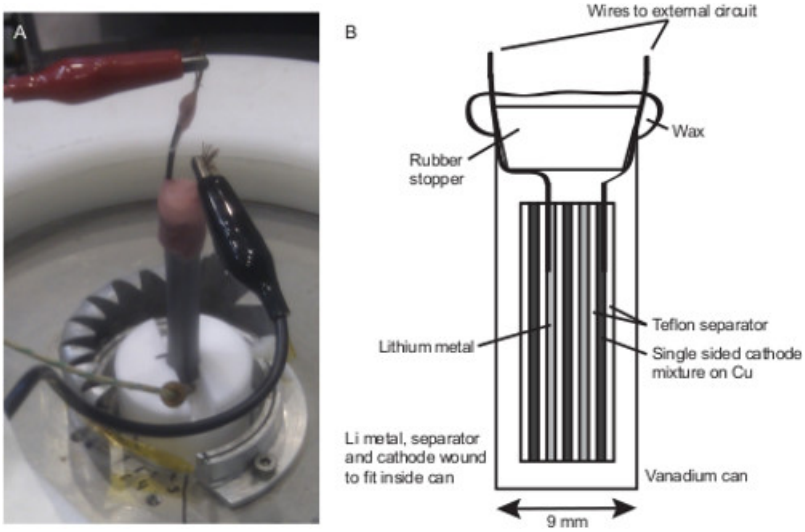

Figure 2: (A): Photo of the *in situ* NPD cell on the Wombat beamline at ANSTO. **(B**) Schematic of the *in situ* cell build, showing the layers that result from the "roll-over" design. Please click here to view a larger version of this figure.

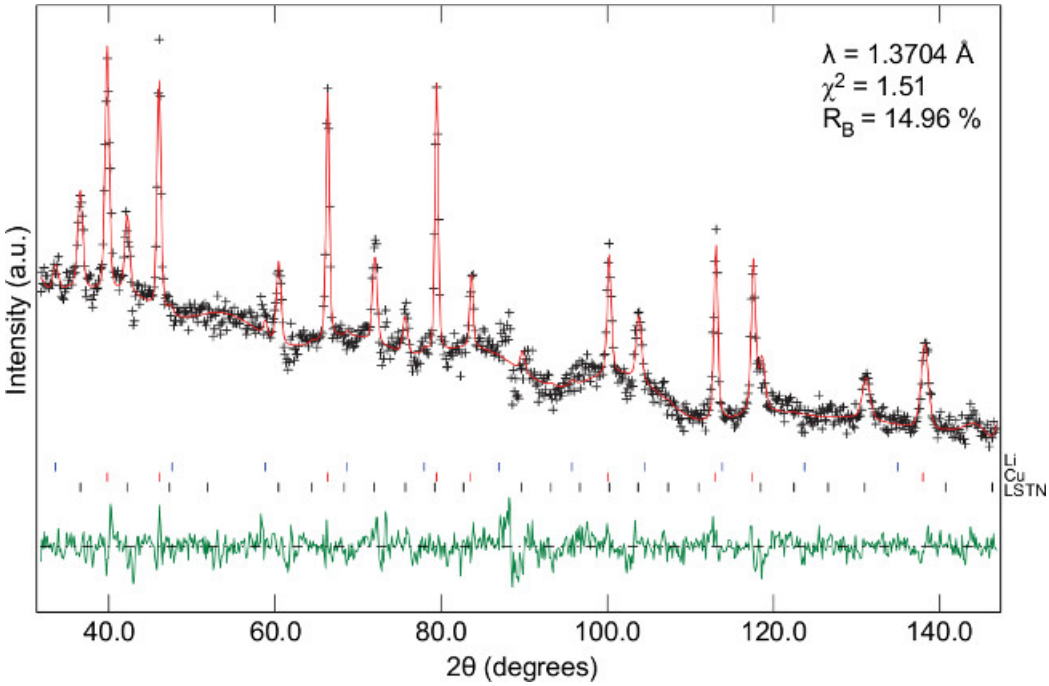

Figure 3: *In situ* NPD pattern of the constructed cell modeled using a multiphase refinement containing $Li_{0.18}Sr_{0.66}Ti_{0.5}Nb_{0.5}O_3$ (LSTN), copper, and lithium. The upper curve corresponds to the model fitted to the data (black crosses) and the lower curve corresponds to the difference between them. Reflection markers are shown as vertical bars. The neutron wavelength (λ), goodness-of-fit (χ^2), and Bragg-R factor (R_B), are given inset.

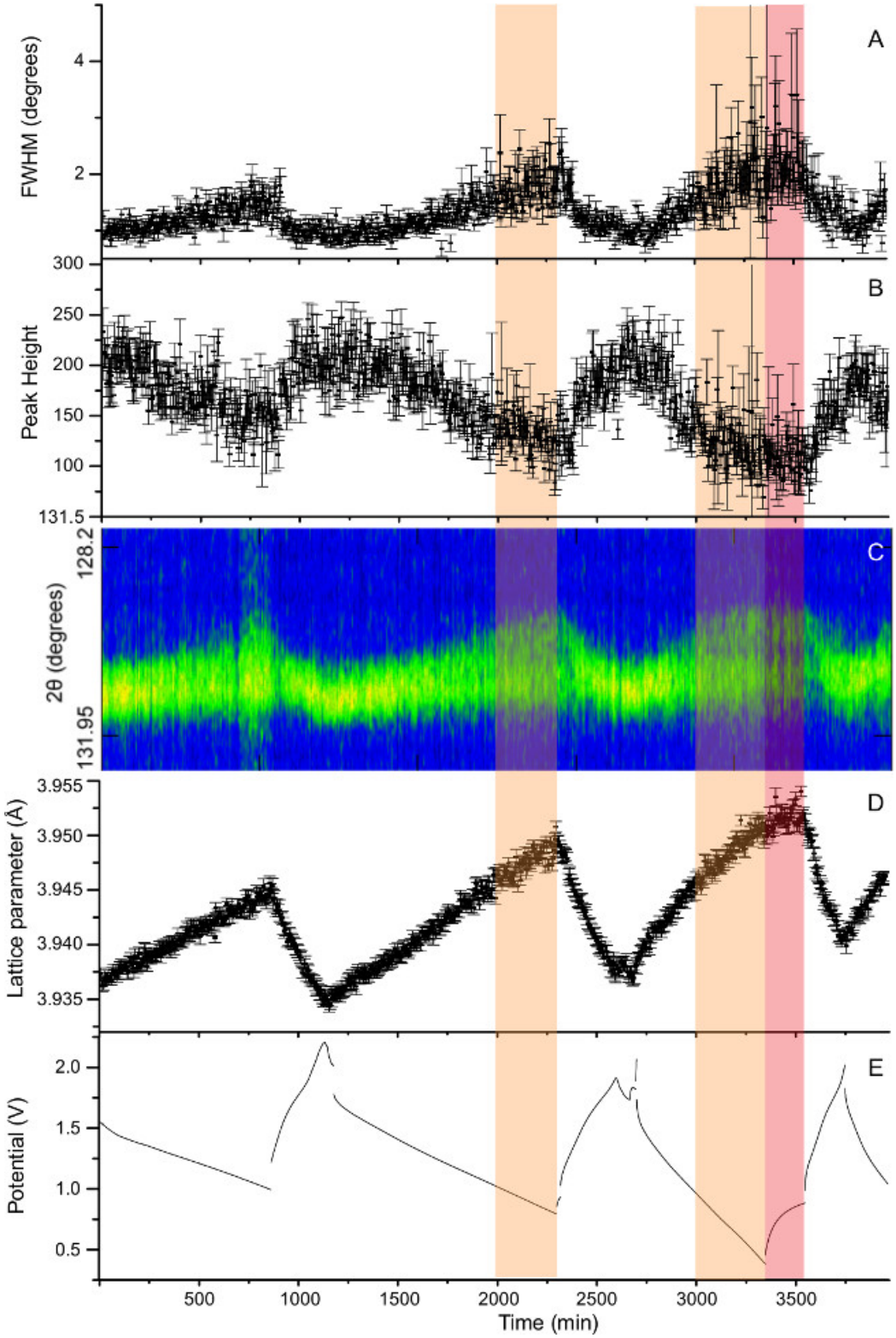

Figure 4: Plots A-C relate to the $Li_{0.18}Sr_{0.66}Ti_{0.5}Nb_{0.5}O_3$ (LSTN) 115 reflection specifically and show the evolution of its shape during cycling. The accuracy of these parameters decreases within the two-phase region as this reflection was modeled with a single pseudo-Voigt function. Plot D shows the variation of the lattice parameter as a function of discharge and plot E shows the battery potential that was collected simultaneously. The orange bars highlight regions where the discharge cycle was taken below 1 V, which also correlates with the onset of the two-phase region. The red bar highlights the region where the cell was allowed to relax and its potential to equilibrate.

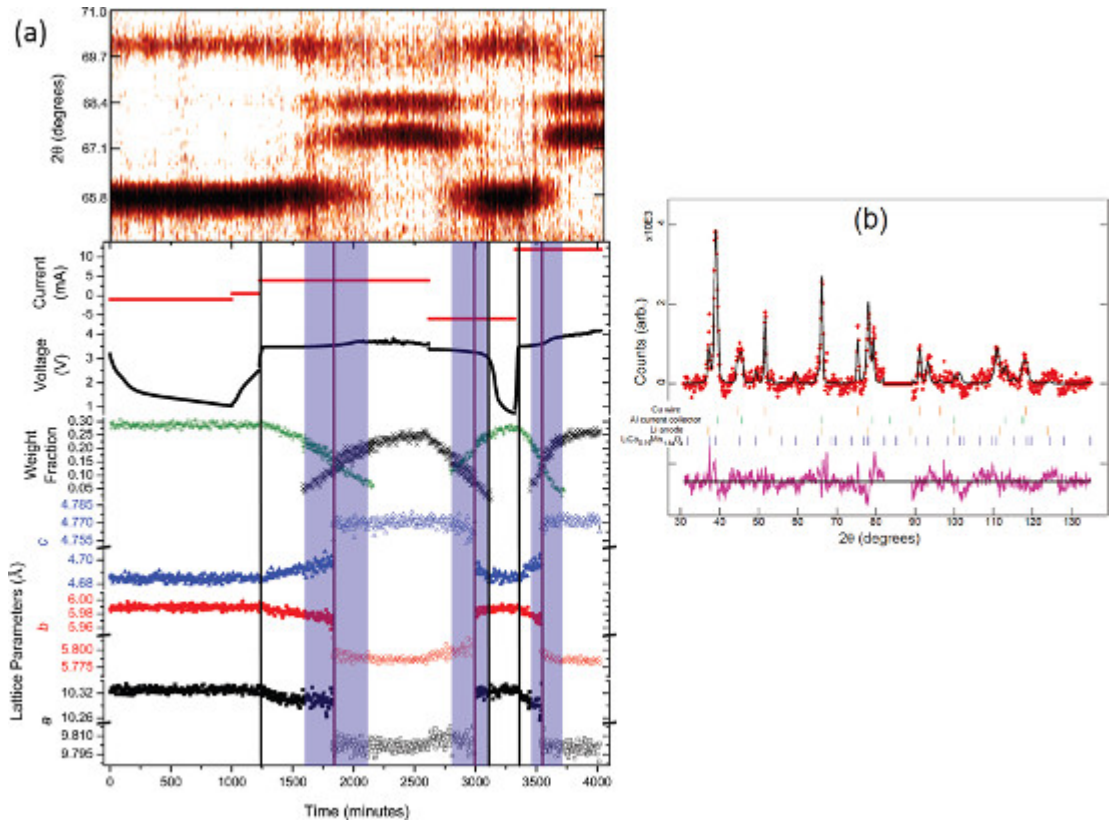

Figure 5: (A) shows the Rietveld-derived lattice parameters and weight fraction of the $LiFePO_4/FePO_4$ cathode, selected 2θ region of the *in situ* NPD data (top) with scaled intensity highlighting the $LiFePO_4$ and $FePO_4$ 221 and 202 reflections, and the current (red). Shaded regions indicate the coexistence of solid solution and two-phase reactions. This figure is reprinted with permission from the Journal of the American Chemical Society **134**, 7867-7873, copyright 2012 American Chemical Society. **(B)** shows *in situ* NDP data of an uncycled cell (red) where, the calculated model for the $Li(Co_{0.16}Mn_{1.84})O_4$ cathode as a black solid line, the difference between the data and the model calculation as a purple line at the bottom, and vertical lines represent reflection markers for the modeled phases. This figure is reprinted with permission from the Journal of Physical Chemistry C **115**, 21473-21480, copyright 2011 American Chemical Society. Please click here to view a larger version of this figure.

Full-Cell Pre-discharge, Pm3m, a = 3.9368(5) Å						
χ^2 = 1.51, R_B = 14.96%						
Atom	Site	x	y	z	Occupancy	U_{iso} (Å^2)
Sr	1b	0.5	0.5	0.5	0.66	0.0079
Ti	1a	0	0	0	0.5	0.0098
Nb	1a	0	0	0	0.5	0.0098
O	3d	0.5	0	0	1	0.006(2)

Table 1: Refined lattice parameter, space group, positional parameters and Debye-Waller factors for $Li_{0.18}Sr_{0.66}Ti_{0.5}Nb_{0.5}O_3$ in the *in situ* cell prior to discharge.

Step	**Current**	**Potential**
	(mA g^{-1})	**(V)**
1	-2.5	1
2	5.0	2
3	-2.5	0.93
4	5.0	1.73
5	12	1.82
6	-3.8	0.38
7	Rest (300 min)	
8	7.5	2

9	-3.8	1.04

Table 2: The electrochemical procedure followed during the *in situ* experiment performed on $Li_{0.18}Sr_{0.66}Ti_{0.5}Nb_{0.5}O_3$.

Discussion

When designing and performing an *in situ* experiment, either with the "roll-over" neutron diffraction cell or another design, there are a number of aspects that must be carefully controlled to ensure a successful experiment. These include careful choice of the type and quantity of cell components, ensuring that the prepared electrode and final constructed cell are of high quality, choosing appropriate diffraction conditions, planning the electrochemical cycling steps to be performed in advance, and finally understanding what the resulting data can and cannot tell one about the material being investigated.

The choice of cell components is vital to ensuring that the resulting diffraction pattern is able to be accurately modeled. In particular, minimizing the number of different phases present will reduce the complexity of the multiphase model. For instance, in the example here the binder used in the positive electrode mixture was PVDF and the separator was polyethylene. However, if the separator used was a PVDF membrane, the total number of components in the cell could have been reduced, simplifying analysis. Additionally, PVDF would decrease the total quantity of hydrogen in the cell, reducing the background contribution. Reducing the quantity of hydrogen containing materials in the cell is the reason why highly expensive deuterated electrolytes are employed for *in situ* NPD. Another alternative would be to replace both the binder in the positive electrode mixture and the separator with hydrogen-free materials (*e.g.* polytetrafluoroethylene). However, depending on the separator material, a larger volume of electrolyte may be required, rapidly increasing the cost of the cell. For example, glass fiber separator, which is hydrogen free, requires far more electrolyte than thin PVDF membranes or polyethylene-based sheets because of its comparatively larger volume. Glass fiber separators are also very difficult to roll.

The ability to prepare a high-quality electrode is essential to ensure that a large quantity of active material is in the beam, allowing fast cycling to be performed and ensuring that the electrode mixture does not detach from the current collector during the rolling process. In the first stage of preparing an electrode film, the positive electrode mixture is added to NMP to form a slurry. The consistency of this slurry is controlled through the mass ratio of NMP to electrode mixture. Obtaining a slurry of the appropriate consistency is essential for preparing a high quality electrode film, especially films that are both stable and large enough for *in situ* NPD. However, achieving the correct consistency may require a lot of testing as the quantity of NMP required is dependent on the morphology and particle size of the active electrode material. Fortunately, this step can be simplified greatly by ball-milling the NMP-electrode slurry. In this case the ratio of NMP to electrode powder mixture becomes less vital and a high-quality film can be readily prepared as long as the ball-milled slurry is spread into a film immediately. The reader is encouraged to also view the previously-reported recommended procedures for preparing a high-quality film.[31] In this report the importance of pressing the electrodes prior to use is emphasized. In the case of the longer electrodes required for *in situ* NPD, applying homogeneous pressure to the entire electrode is best achieved using a rolling press. However, if a rolling press is not available, a flat-plate press can be used. Finally, the "roll-over" *in situ* cell design is compatible with a double-sided positive electrode without any additional changes made during construction. Using a double-sided electrode effectively doubles the quantity of the active material relative to the other battery components, leading to a higher quality diffraction pattern.

A common difficulty encountered is obtaining good pressure applied to the entire battery roll in the constructed cell. This can result in poor or inhomogeneous ionic diffusion through the cell, as shown for the $Li_{0.18}Sr_{0.66}Ti_{0.5}Nb_{0.5}O_3$ results above, or a cell that does not function. Obtaining good pressure across to the stack is particularly difficult when winding the cell by hand. The process involves manual dexterity inside a glovebox and may not lead to consistent results. These difficulties can be overcome by using an automatic cell winding machine, although the amount of sample required may increase. Finally, the total mass of all cell components in the cell must be recorded in order to calculate the total neutron absorption. Without an appropriate absorption correction structural parameters, such as the atomic displacement parameters (ADPs), may refine to unrealistic values. In general it is good practice to measure and apply an appropriate absorption correction for NPD experiments.

Prior to beginning the *in situ* NPD experiment several experimental conditions must be considered and set. For example, the resulting angular resolution must be appropriate for the material investigated. If an electrode crystal structure adopts a low-symmetry space group reflections may not be resolved due to overlap with reflections from the same phase or the other phases present in the cell. To resolve certain reflections the wavelength of neutrons impinging on the sample may need to be adjusted, *e.g.* longer wavelengths can separate reflections in 2. Unfortunately, this reduces the Q-space range probed. This was potentially an issue for the $Li_{0.18}Sr_{0.66}Ti_{0.5}Nb_{0.5}O_3$ results reported above. In this case reflections from planes with smaller *d*-spacings were previously determined to provide information of lithium ordering, and thus a shorter wavelength was selected. However, this also made it difficult to resolve the peak splitting due to the appearance of the second phase.

In addition to choosing the appropriate set of experimental parameters for the neutron diffractometer, the electrochemical cycling conditions should be pre-determined and not changed dramatically during the experiment. During cell cycling it is likely that the material exists in a metastable state which can subsequently relax once the cell is disconnected. If this is a particular property of the material which is being investigated then there should not be any issues, however, if the aim of the experiment is to investigate the rate of change of some structural parameter during charge or discharge then interruptions and the subsequent structural relaxation may influence the outcome. In addition, avoiding interruptions also simplifies the resulting sequential refinement by avoiding the need to restart the refinement at every break. It is also recommended that if the experimenter aims to determine the lithium position and occupancy at various stages of discharge then longer data collections at the end of each charge and discharge cycle is advised with an appropriate equilibration electrochemical step. The longer data collections may ensure that there is sufficient signal-to-noise to improve the chances of observing and modeling the lithium in addition to serving as a benchmark for how the lithium changes during cycling.

Once the data have been collected then there are a number of analysis methods which can be employed depending on the desired outcome of the experiment. Usually, the best form of analysis is Rietveld refinement with few constraints, although this is more difficult to perform than either a refinement with several constraints (such as fixed atomic co-ordinates, occupancies, or ADPs) or modeling the changes of a single reflection.

Occasionally the information obtained from a more simple analysis is all that is desired from an *in situ* experiment, and so performing a more complex unconstrained Rietveld refinement is unnecessary.

To best judge what may be able to be accurately modeled during a sequential Rietveld refinement an initial refinement using a single dataset collected for a long period prior to discharge is often necessary. As was the case for $Li_{0.18}Sr_{0.66}Ti_{0.5}Nb_{0.5}O_3$, if certain parameters are unable to be accurately determined in the initial refinement, it is unlikely that they will be accurately determined during the sequential refinement. However, being able to perform a successful sequential Rietveld refinement is one of the most desirable outcomes of an *in situ* NPD experiment. As the model is refined against every point within the diffraction pattern, highly accurate information of the change in the average structure for all phases during electrochemical cycling can be extracted and directly correlated to the potential profile. In addition, if rapid data collection was performed the rate of structural change during battery cycling can be investigated and the kinetics of lithium insertion determined. Obtaining a stable refinement with few constraints, such as fixing atomic co-ordinates, occupancies, and ADPs, requires high-quality data with good signal-to-noise, high angular-resolution, and access to a large *d*-space range. The specific data quality required depends in part on the material being investigated. For example, a more complex structure will need higher signal-to-noise to see weaker reflections and higher resolution in order to observe peak splitting. Thus, occasionally constraints may be necessary, as was the case for $Li_{0.18}Sr_{0.66}Ti_{0.5}Nb_{0.5}O_3$, where certain parameters are held constant during a refinement. In addition, caution must always be taken to ensure that the resulting model is chemically reasonable. This can be performed by checking the visual fit of the model to the data to ensure that there are no systematic differences, checking that the refined parameters are physically reasonable, as well as monitoring the statistical measures of the quality of fit (such as R_B or χ^2). The observation of reproducible trends in the parameters between several electrochemical cycles can add more weight to a particular observation.

In addition to performing a Rietveld refinement using the data, changes occurring to characteristic reflections during battery cycling can be modeled.[8,18,19] This is particularly useful if it is known in advance which reflections are influenced by either lithium ordering or a change in the host structure. The changes to these characteristic reflections can then be correlated to changes in the electrochemical potential-profile to build an understanding of structure-property relationships. The change in position or integrated intensity of a specific reflection can be modeled using programs such as LAMP[33] or Origin. Finally, the appearance of characteristic reflections indicating the formation of new phases can be followed during electrochemical cycling.[8,16,35,36] Similar to other changes observed *in situ*, their appearance and identity can be linked to the observed electrochemical properties. The reader is encouraged to view and read the article about *in situ* X-ray based studies by see Doeff *et al.*[37]

No matter what form of analysis is performed, if data were collected continuously during electrochemical cycling, information unique to *in situ* diffraction will be obtained. In particular, information regarding the formation of metastable phases and non-equilibrium processes from the whole cell can be extracted.[11,28,29] Results for example cathode materials studied as a function of charge/discharge using *in situ* NPD cells are shown in **Figure 5**. **Figure 5A** shows a selected region of the *in situ* NPD patterns, voltage profiles, weight fractions, and lattice parameters of the active cathode material, $LiFePO_4$ and $FePO_4$.[25] While **Figure 5B** shows a typical multiphase refinement using structural models of the components and an *in situ* NPD dataset.[26]

In situ NPD is a tool that is sensitive to lithium, the charge carrier in lithium-ion batteries. Thus, there is lithium-sensitive insight gained into the function of electrodes during battery operation. Charging processes can be related to how the electrode crystal-structure expands/contracts/forms new phases and to how lithium inserts/extracts from these electrodes. *In situ* NPD can uncover how lithium is inserted/extracted into electrodes, via one, two, or more crystallographic sites, and this directly influences the ease of charging/discharging a whole battery. By determining how and where lithium is inserted/extracted we can design new materials that can take advantage of this knowledge. For example, materials with larger voids for lithium to reside in can be designed such that more lithium can be inserted, leading to higher capacity batteries. In addition, knowledge of the crystallographic sites that lithium occupies during insertion/extraction can be used to direct the development of materials with larger 'tunnels' for lithium, again potentially allowing more lithium to be reversibly inserted/extracted, especially at higher rates of discharge/charge. Although, these examples are based on insertion electrodes, *in situ* NPD may in the future provide valuable information for electrodes that undergo conversion reactions. Therefore, *in situ* NPD provides crucial information on electrode function that can be used to design the next generation of electrodes.

Future in situ NPD studies will tackle more complex systems, exhibiting lower symmetry space-groups and/or more complex lithium distributions. Additionally, these studies can be used to develop new materials for alternative applications — why use an electrode for a battery? We can use an electrode as a starting material, insert/extract a known amount of lithium (with information provided by *in situ* NPD), extract the electrode and use it for another application, *e.g.* taking advantage of another physical property. Further, electrochemical cells can be developed that allow *in situ* NPD to probe structural information on the processes occurring in speciation cells, lithium-air batteries, and fuel cells. Performing reactions *in situ* allows us to study functioning materials, and this is underpinned by having appropriate cells that merge the requirements of electrochemistry and structural characterization.

Disclosures

The authors have nothing to disclose.

Acknowledgements

We thank AINSE Ltd for providing support through the research fellowship and postgraduate award scheme.

References

1. Winter, M., Besenhard, J. O., Spahr, M. E., & Novak, P. Insertion electrode materials for rechargeable lithium batteries. *Adv. Mater. (Weinheim, Ger.).* **10**, 725-763, doi:10.1002/(sici)1521-4095(199807)10:10<725::aid-adma725>3.0.co;2-z (1998).
2. Wakihara, M. Recent developments in lithium ion batteries. *Mater. Sci. Eng., R.* **R33**, 109-134, doi:10.1016/s0927-796x(01)00030-4 (2001).
3. Goodenough, J. B., & Kim, Y. Challenges for Rechargeable Li Batteries. *Chem. Mater.* **22**, 587-603, doi:10.1021/cm901452z (2010).

4. Palomares, V. *et al.* Na-ion batteries, recent advances and present challenges to become low cost energy storage systems. *Energy Environ. Sci.* **5**, 5884-5901, doi:10.1039/c2ee02781j (2012).
5. Masquelier, C., & Croguennec, L. Polyanionic (phosphates, silicates, sulfates) frameworks as electrode materials for rechargeable Li (or Na) batteries. *Chem. Rev. (Washington, DC, U. S.).* **113**, 6552-6591, doi:10.1021/cr3001862 (2013).
6. Reddy, M. V., Subba Rao, G. V., & Chowdari, B. V. R. Metal Oxides and Oxysalts as Anode Materials for Li Ion Batteries. *Chem. Rev. (Washington, DC, U. S.).* **113**, 5364-5457, doi:10.1021/cr3001884 (2013).
7. Goodenough, J. B., & Kim, Y. Challenges for rechargeable batteries. *J. Power Sources.* **196**, 6688-6694, doi:10.1016/j.jpowsour.2010.11.074 (2011).
8. Sharma, N., & Peterson, V. K. Overcharging a lithium-ion battery: Effect on the Li_xC_6 negative electrode determined by *in situ* neutron diffraction. *J. Power Sources.* **244**, 695-701, doi:10.1016/j.jpowsour.2012.12.019 (2013).
9. Sharma, N. *et al.* Structural changes in a commercial lithium-ion battery during electrochemical cycling: An *in situ* neutron diffraction study. *J. Power Sources.* **195**, 8258-8266, doi:10.1016/j.jpowsour.2010.06.114 (2010).
10. Senyshyn, A., Muehlbauer, M. J., Nikolowski, K., Pirling, T., & Ehrenberg, H. 'In-operando' neutron scattering studies on Li-ion batteries. *J. Power Sources.* **203**, 126-129, doi:10.1016/j.jpowsour.2011.12.007 (2012).
11. Sharma, N., Yu, D., Zhu, Y., Wu, Y., & Peterson, V. K. Non-equilibrium Structural Evolution of the Lithium-Rich $Li_{1+y}Mn_2O_4$ Cathode within a Battery. *Chemistry of Materials.* **25**, 754-760, doi:10.1021/cm303851w (2013).
12. Pang, W. K., Sharma, N., Peterson, V. K., Shiu, J. J., & Wu, S. H. *In-situ* neutron diffraction study of the simultaneous structural evolution of a $LiNi_{0.5}Mn_{1.5}O_4$ cathode and a $Li_4Ti_5O_{12}$ anode in a $LiNi_{0.5}Mn_{1.5}O_4$ parallel to $Li_4Ti_5O_{12}$ full cell. *Journal of Power Sources.* **246**, 464-472, doi:10.1016/j.jpowsour.2013.07.114 (2014).
13. Pang, W. K., Peterson, V. K., Sharma, N., Shiu, J.-J., & Wu, S.-h. Lithium Migration in $Li_4Ti_5O_{12}$ Studied Using *in Situ* Neutron Powder Diffraction. *Chem. Mater.* **26**, 2318-2326, doi:10.1021/cm5002779 (2014).
14. Bergstom, O., Andersson, A. M., Edstrom, K., & Gustafsson, T. A neutron diffraction cell for studying lithium-insertion processes in electrode materials. *J. Appl. Crystallogr.* **31**, 823-825, doi:10.1107/s002188989800538x (1998).
15. Sharma, N., Du, G. D., Studer, A. J., Guo, Z. P., & Peterson, V. K. *In-situ* neutron diffraction study of the MoS_2 anode using a custom-built Li-ion battery. *Solid State Ion.* **199**, 37-43, doi:10.1016/j.ssi.2011.07.015 (2011).
16. Sharma, N., & Peterson, V. K. Current-dependent electrode lattice fluctuations and anode phase evolution in a lithium-ion battery investigated by *in situ* neutron diffraction. *Electrochim. Acta.* **101**, 79-85, doi:10.1016/j.electacta.2012.09.101 (2013).
17. Dolotko, O., Senyshyn, A., Muhlbauer, M. J., Nikolowski, K., & Ehrenberg, H. Understanding structural changes in NMC Li-ion cells by *in situ* neutron diffraction. *Journal of Power Sources.* **255**, 197-203, doi:10.1016/j.jpowsour.2014.01.010 (2014).
18. Rodriguez, M. A., Ingersoll, D., Vogel, S. C., & Williams, D. J. Simultaneous In Situ Neutron Diffraction Studies of the Anode and Cathode in a Lithium-Ion Cell. *Electrochem. Solid-State Lett.* **7**, A8-A10, doi:10.1149/1.1628664 (2004).
19. Wang, X.-L. *et al.* Visualizing the chemistry and structure dynamics in lithium-ion batteries by *in-situ* neutron diffraction. *Sci. Rep.* **2**, srep00747, 00747 pp., doi:10.1038/srep00747 (2012).
20. Rodriguez, M. A., Van Benthem, M. H., Ingersoll, D., Vogel, S. C., & Reiche, H. M. *In situ* analysis of $LiFePO_4$ batteries: Signal extraction by multivariate analysis. *Powder Diffr.* **25**, 143-148, doi:10.1154/1.3393786 (2010).
21. Berg, H., Rundlov, H., & Thomas, J. O. The $LiMn_2O_4$ to lambda-MnO_2 phase transition studied by *in situ* neutron diffraction. *Solid State Ion.* **144**, 65-69, doi:10.1016/s0167-2738(01)00894-3 (2001).
22. Roberts, M. *et al.* Design of a new lithium ion battery test cell for *in-situ* neutron diffraction measurements. *Journal of Power Sources.* **226**, 249-255, doi:10.1016/j.jpowsour.2012.10.085 (2013).
23. Rosciano, F., Holzapfel, M., Scheifele, W., & Novak, P. A novel electrochemical cell for *in situ* neutron diffraction studies of electrode materials for lithium-ion batteries. *J. Appl. Crystallogr.* **41**, 690-694, doi:10.1107/s0021889808018025 (2008).
24. Godbole, V. A. *et al.* Circular *in situ* neutron powder diffraction cell for study of reaction mechanism in electrode materials for Li-ion batteries. *RSC Adv.* **3**, 757-763, doi:10.1039/c2ra21526h (2013).
25. Colin, J.-F., Godbole, V., & Novak, P. *In situ* neutron diffraction study of Li insertion in $Li_4Ti_5O_{12}$. *Electrochem. Commun.* **12**, 804-807, doi:10.1016/j.elecom.2010.03.038 (2010).
26. Bianchini, M. *et al.* A New Null Matrix Electrochemical Cell for Rietveld Refinements of *In-Situ* or Operando Neutron Powder Diffraction Data. *Journal of the Electrochemical Society.* **160**, A2176-A2183, doi:10.1149/2.076311jes (2013).
27. Liu, H. D., Fell, C. R., An, K., Cai, L., & Meng, Y. S. *In-situ* neutron diffraction study of the xLi(2)MnO(3)center dot(1-x)$LiMO_2$ (x=0, 0.5; M = Ni, Mn, Co) layered oxide compounds during electrochemical cycling. *Journal of Power Sources.* **240**, 772-778, doi:10.1016/j.jpowsour.2013.04.149 (2013).
28. Sharma, N. *et al.* Direct Evidence of Concurrent Solid-Solution and Two-Phase Reactions and the Nonequilibrium Structural Evolution of $LiFePO_4$. *J. Am. Chem. Soc.* **134**, 7867-7873, doi:10.1021/ja301187u (2012).
29. Sharma, N. *et al.* Time-Dependent *in-Situ* Neutron Diffraction Investigation of a $Li(Co_{0.16}Mn_{1.84})O_4$ Cathode. *J. Phys. Chem. C.* **115**, 21473-21480, doi:10.1021/jp2026237 (2011).
30. Du, G. *et al.* Br-Doped $Li_4Ti_5O_{12}$ and Composite TiO_2 Anodes for Li-ion Batteries: Synchrotron X-Ray and *in situ* Neutron Diffraction Studies. *Adv. Funct. Mater.* **21**, 3990-3997, doi:10.1002/adfm.201100846 (2011).
31. Marks, T., Trussler, S., Smith, A. J., Xiong, D., & Dahn, J. R. A Guide to Li-Ion Coin-Cell Electrode Making for Academic Researchers. *J. Electrochem. Soc.* **158**, A51-A57, doi:10.1149/1.3515072 (2010).
32. Brant, W. R. *et al.* Rapid Lithium Insertion and Location of Mobile Lithium in the Defect Perovskite $Li_{0.18}Sr_{0.66}Ti_{0.5}Nb_{0.5}O_3$. *ChemPhysChem.* **13**, 2293-2296 (2012).
33. Richard, D., Ferrand, M., & Kearley, G. J. Analysis and Visualisation of Neutron-Scattering Data. *J. Neutron Research.* **4**, 33-39 (1996).
34. Brant, W. R., Schmid, S., Du, G., Gu, Q., & Sharma, N. A simple electrochemical cell for *in-situ* fundamental structural analysis using synchrotron X-ray powder diffraction. *Journal of Power Sources.* **244**, 109 - 114, doi:http://dx.doi.org/10.1016/j.jpowsour.2013.03.086 (2013).
35. Hu, C.-W. *et al.* Real-time investigation of the structural evolution of electrodes in a commercial lithium-ion battery containing a V-added $LiFePO_4$ cathode using *in-situ* neutron powder diffraction. *J. Power Sources.* **244**, 158-163, doi:10.1016/j.jpowsour.2013.02.074 (2013).
36. Cai, L., An, K., Feng, Z., Liang, C., & Harris, S. J. *In-situ* observation of inhomogeneous degradation in large format Li-ion cells by neutron diffraction. *J. Power Sources.* **236**, 163-168, doi:10.1016/j.jpowsour.2013.02.066 (2013).
37. Doeff, M. M. *et al.* Characterization of electrode materials for lithium ion and sodium ion batteries using synchrotron radiation techniques. *J. Visualized Exp.*, e50594/50591-e50594/50599, 50599 pp., doi:10.3791/50594 (2013).

